Journal of Colloid and Interface Science 570 (2020) 300–311

Contents lists available at ScienceDirect

Journal of Colloid and Interface Science

journal homepage: www.elsevier.com/locate/jcis

Highly dispersed Pt nanoparticles on ultrasmall EMT zeolite: A peroxidase-mimic nanoenzyme for detection of H_2O_2 or glucose

Xiaolong Li [a,b,1], Xuanyu Yang [b,1], Xiaowei Cheng [b,*], Yuye Zhao [c], Wei Luo [c,*], Ahmed A. Elzatahry [d], Abdulaziz Alghamdi [e], Xing He [a], Jiacan Su [f], Yonghui Deng [b,g]

[a] School of Materials Science and Engineering, University of Shanghai for Science and Technology, Shanghai 200093, China
[b] Department of Chemistry, Shanghai Key Laboratory of Molecular Catalysis and Innovative Materials, Fudan University, Shanghai 200433, China
[c] State Key Laboratory for Modification of Chemical Fibers and Polymer Materials, College of Materials Science and Engineering, Institute of Functional Materials, Donghua University, Shanghai 201620, China
[d] Materials Science and Technology Program, College of Arts and Sciences, Qatar University, PO Box 2713, Doha, Qatar
[e] Department of Chemistry, College of Science, King Saud University, PO Box 2455, Riyadh 11451, Saudi Arabia
[f] Department of Trauma Orthopaedics, Changhai Hospital, Second Military Medical University, Shanghai 200433, China
[g] State Key Lab of Transducer Technology, Shanghai Institute of Microsystem and Information Technology, Chinese Academy of Sciences, Shanghai 200050, China

GRAPHICAL ABSTRACT

Hybrid Pt/EMT nanomaterials in size of about 15–20 nm were synthesized by highly dispersing Pt nanoparticles (5–8 nm) on the support of ultrasmall EMT zeolite, which were utilized as peroxidase mimics for accurate detection of H_2O_2 and glucose with a sensitive and reliable colorimetric assay, based on the catalytic oxidation of colorless TMB into blue ox-TMB using uniformly loaded Pt nanoparticles as active sites on microporous EMT zeolite with large surface area and pore volume.

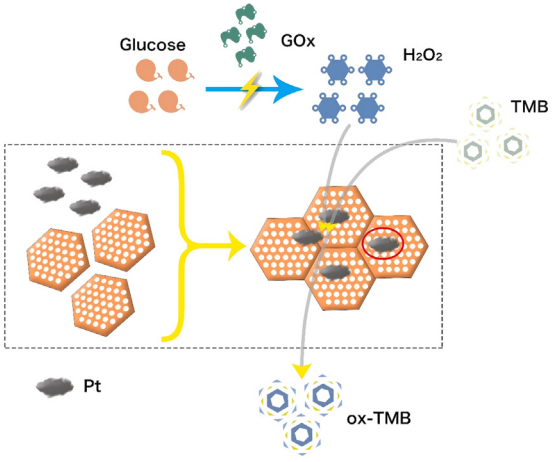

ARTICLE INFO

Article history:
Received 21 January 2020
Revised 28 February 2020

ABSTRACT

In past decade, Pt-based nanomaterials as peroxidase mimics have attracted much attention for H_2O_2 and glucose detection. However, easy aggregation of Pt nanoparticles (Pt NPs) greatly decreases their peroxidase-like activity. In this work, novel Pt/EMT nanocomposites were prepared by uniformly loading

* Corresponding authors at: Department of Chemistry, Shanghai Key Laboratory of Molecular Catalysis and Innovative Materials, Fudan University, Shanghai 200433, China (X. Cheng).
E-mail addresses: xwcheng@fudan.edu.cn (X. Cheng), wluo@dhu.edu.cn (W. Luo).
[1] These authors contributed equally to this work.

https://doi.org/10.1016/j.jcis.2020.02.118

Accepted 28 February 2020
Available online 3 March 2020

Keywords:
Pt/EMT nanocomposite
Zeolite
Peroxidase mimic
Colorimetric assay
Glucose detection

Pt NPs (5–8 nm) onto the support of ultrasmall EMT zeolite (15–20 nm), a kind of low-silica microporous aluminosilicate material. The hybrid Pt/EMT nanomaterials could be well dispersed in water to form a homogeneous suspension, and were then utilized as a superior peroxidase-like catalyst for oxidation of 3,3′,5,5′-tetramethylbenzidine (TMB) in the presence of hydrogen peroxide (H_2O_2). The optimal catalyst of 2.6Pt/EMT nanocomposite exhibited excellent catalytic performance toward H_2O_2 and TMB than natural enzyme of horseradish peroxidase (HRP) by using a steady-state kinetic analysis based on the typical Michaelis-Menten kinetics theory. The peroxidase-like catalyst showed a promising activity in a wide pH and temperature range as well as the long-term stability. A facile and reliable colorimetric assay based on the peroxidase mimic of Pt/EMT nanocomposite was constructed for precise detection of H_2O_2 and glucose in a wide linear range, with low limits of detection of 1.1 μM and 13.2 μM, respectively. Due to high selectivity to glucose against other sugars on the catalyst, the method was demonstrated to accurately measure the concentration of glucose in real samples including human blood serum and fruit juices, indicating a potential application of the Pt/EMT nanocomposites as a robust peroxidase mimic and a reliable biosensor in the fields of clinical diagnosis, pharmaceutical, food research and so on.

1. Introduction

Since the first report about the intrinsic enzyme activity of Fe_3O_4 nanoparticles (NPs) in 2007 [1], the research about artificial enzyme mimics based on inorganic nanomaterials has attracted more and more interests in biochemical and bioassay applications, because of their evident advantages over natural enzymes, including high efficiency, good stability, facile preparation, low cost and so on [2–7]. Over the past decade, a great number of inorganic nanomaterials with diverse structures and compositions, such as metal oxides [8], noble metals [9], metal sulfides [10], etc., have been rationally designed as enzyme mimics in peroxidase-like catalytic reactions. Platinum (Pt) is one of the most common noble metals widely used as the catalyst in chemical process, which is also extensively considered to be a promising peroxidase mimic candidate. However, the drawbacks of high cost and easy deactivation caused by Pt aggregation greatly limit its application [11]. Until now it has not been largely explored in practical biological area. One strategy to overcome these drawbacks is to precisely control the size and morphology of Pt nanomaterials to achieve superior enzymatic activities, such as ultrasmall Pt nanoclusters [12], porous Pt nanotubes [13], cubic Pt nanocrystals [14], irregular-shaped Pt NPs [15], etc. The other strategy is based on the synthesis of Pt/support composite nanomaterials with well-designed stable structure and multi-functionality, which are usually achieved through uniform dispersion of Pt NPs on appropriate supports, including Pt/CeO_2 nanocomposites [16], Au@Pt core-shell nanorods [17], dumbbell-like PtPd-Fe_3O_4 NPs [18], ferritin-Pt NPs [19], dendrimer-encapsulated Pt NPs [20], mesoporous silica encapsulated Pt NPs [21], and so on. Despite that these Pt-loaded hybrid nanocomposites show satisfactory performance as peroxidase mimics, it still remains a great challenge to obtain the high-quality supports in a low-cost way and realize highly uniform dispersion of Pt NPs on them.

Different from mesoporous materials (e.g., mesoporous SiO_2), zeolite is a kind of crystalline aluminosilicates with regular micropores (pore size < 2 nm) interconnected with well-developed channels, showing stable framework structure, favorable surface Brönsted/Lewis acidity and shape selectivity [22–26]. Usually most zeolites, such as ZSM-5 (MFI), SSZ-13 (CHA), beta (BEA), etc., can be conveniently synthesized by a traditional hydrothermal method, and thus they are being widely utilized as low-cost industrial catalysts or catalyst supports in large scale [27–29]. In recent years, the research about nanosized zeolites and mesoporous zeolites has attracted great attention, because they can overcome the diffusion limitation within micropores and improve transport/accessibility of reactants to the active sites [30–34]. Although a great number of nanosized zeolites have been reported, there still remains a great difficulty to obtain ultrasmall zeolite nanocrystals (<20 nm) by a template-free method [35,36]. Quite recently, through precisely controlling the nucleation kinetics at low temperature (30 °C), Mintova and co-workers synthesized ultrasmall zeolite materials including EMT (10–20 nm) and Y (10–70 nm) from template-free colloidal precursors [35,37], both of which have 3-dimensional 12-membered ring channel system, and they can be highly dispersed in water to form homogeneous suspensions. Beside the excellent performance as catalysts like zeolite Y in isomerization, alkylation and aromatization reactions, EMT zeolite can also be used as an ideal host for silver nanoparticles through introduction of silver ions and subsequent reduction, mainly due to its low Si/Al ratio, high porosity and large pore size [38]. In addition, these nanosized Ag-EMT zeolites were stabilized in aqueous suspensions for long-term antibacterial applications. To the best of our knowledge, this kind of zeolite with ultrasmall size and high dispersion in aqueous solution has not been developed as the support of enzyme mimics in peroxidase-like reactions. Based on the typical properties of large surface area, surface acidity and hydrophilicity of zeolite Y, we recently synthesized a CeO_2/Y hybrid nanocomposite through uniformly decorating CeO_2 NPs on external surface of commercial zeolite Y as support. This hybrid material was then established as a peroxidase-like catalyst for the first time, showing high catalytic activity, low limit of detection and long-term stability toward TMB oxidation in presence of H_2O_2, due to the synergistic effects of outstanding activity of CeO_2 NPs and high surface area of zeolite Y as a support [39]. Therefore, we strongly believe that the nanosized Pt/EMT zeolites could also be used as a high-performance enzyme mimic because of its intrinsic surface acidity, ultrasmall particle size, uniform dispersion of Pt NPs and homogeneous suspension characteristics in water.

Herein, we first prepared highly-crystallized EMT zeolite in ultrasmall size of 15–20 nm. Hybrid Pt/EMT nanocomposites with highly dispersed Pt NPs (5–8 nm) on the ultrasmall EMT zeolite were successfully synthesized through a facile wet impregnation method combined with $NaBH_4$ in situ reduction route. The Pt/EMT nanocatalysts exhibited superior peroxidase-mimicking activity and catalytic stability toward TMB oxidation in the presence of H_2O_2 in comparison with EMT zeolite itself and Pt/Y catalyst. A sensitive and reliable colorimetric assay was set up to precisely determine the concentration of H_2O_2 and glucose in buffer solution and practical samples (human blood serum and fruit juices) with a wide linear range and low limits of detection (1.1 μM for H_2O_2 and 13.2 μM for glucose). The excellent catalytic activity/selectivity, high long-term stability, and facile synthesis in low cost of this

kind of peroxidase mimics endow them with a promising potential as the commercial glucose detectors and biosensors in the wide application of some real physiological samples.

2. Experimental section

2.1. Chemicals and materials

The chemicals of sodium aluminate ($NaAlO_2$), sodium hydroxide (NaOH), sodium borohydride ($NaBH_4$), chloroplatinic acid hexahydrate ($H_2PtCl_6{\cdot}6H_2O$), hydrogen peroxide (H_2O_2, 30 wt%), 3,3′,5,5′-tetramethylbenzidine (TMB), sodium acetate (NaAc), acetic acid (HAc), glucose, sucrose, lactose, fructose, glucose oxidase (GOx, 2 mg/mL) were purchased from Sinopharm Chemical Reagent Co., Ltd. Colloidal silica (Ludox AS-30, SiO_2 = 30 wt%) was bought from Sigma-Aldrich. All reagents above were of analytical grade and used without further purification. Sodium acetate buffer (0.2 M, pH = 5.5) and phosphate buffer saline (PBS, 0.1 M, pH = 7.4) were freshly prepared before use. Human blood serum was supplied by Changhai Hospital (Shanghai, China). Master Kong Juicy peach beverage and Minute Maid orange juice were purchased from marketplace.

2.2. Synthesis of ultrasmall EMT zeolite

According to the previous report by Mintova and co-workers, the ultrasmall EMT zeolite was synthesized in a template-free colloidal system at low temperature of 303 K [37]. In a typical synthesis of EMT zeolite, solution A was firstly prepared by dissolving 2 g of $NaAlO_2$ in 10 mL of distilled water under stirring. Solution B was prepared by dissolving 17 g of NaOH in 30 mL of distilled water under stirring. Both solutions were thoroughly cooled in an ice bath at 277 K. Then, solution A was slowly poured into solution B under vigorous stirring to form a mixed solution C, in which 10.46 mL of colloidal silica was slowly injected under vigorous stirring. The final turbid suspension was formed with the following chemical compositions: 18.45 Na_2O: 1.0 Al_2O_3: 5.15 SiO_2: 240 H_2O. The suspension was continuously stirred for 5 min and then held in water bath at 303 K for 36 h under sustained stirring. After that the solid product was separated by centrifugation at 8000 r/min for 10 min and then washed with distilled water for several times until pH value of the solution after centrifugation was close to 8. Finally, the solid powder of EMT zeolite was dried in a vacuum oven at room temperature for at least 24 h.

2.3. Preparation of xPt/EMT nanocomposite catalysts

The Pt/EMT nanocomposite catalysts with different contents of Pt (0.65, 1.3, 1.95, 2.6, 3.25, 3.9 wt%, denoted as *x*Pt/EMT catalysts, *x* = mass ratio of Pt to EMT zeolite (%)) were prepared by a method of wet impregnation combined with $NaBH_4$ in situ reduction [40]. In a typical synthesis of 2.6Pt/EMT nanocomposite, 100 mg of EMT zeolite was well dispersed in 15 mL of water by sonication for 20 min to form a homogeneous suspension. Then, 7 mL of H_2PtCl_6 solution (2 mM) was added dropwise with further stirring for 1 h. A freshly prepared $NaBH_4$ solution (0.2 M) of 2 mL was injected dropwise into the mixture at 273 K, followed by stirring at room temperature for 12 h. The solid powder was collected by centrifugation at 6000 r/min for 5 min, and then washed with water and ethanol for 3 times, respectively. Finally, the 2.6Pt/EMT nanocomposite was obtained by drying in a vacuum oven at room temperature overnight. Pt/EMT materials can be recycled after use, which were collected through centrifugation and washing for several times. The materials were further treated by vacuum drying before reuse.

2.4. Peroxidase-like activity investigation of 2.6Pt/EMT catalysts

To investigate the peroxidase-like activity of the as-prepared *x*Pt/EMT catalysts, the catalytic oxidation of the substrate TMB in the presence of H_2O_2 was tested. In a typical process, the peroxidase-mimicking reaction was performed at 298 K by using 0.45 mg of Pt/EMT catalyst in 3 mL of sodium acetate buffer (0.2 M, pH = 5.5) with 200 μL TMB (3 mM) and 100 μL H_2O_2 (100 mM), unless otherwise stated.

For comparison, catalytic activity was tested on parent EMT zeolite or Pt-loaded Y zeolite (2.6Pt/Y, 0.45 mg) as the peroxidase-like catalysts under the same conditions. In a typical process, the peroxidase-mimicking reaction was performed at 298 K by using 0.45 mg of 2.6Pt/Y catalyst in 3 mL of sodium acetate buffer (0.2 M, pH = 5.5) with 200 μL TMB (3 mM) and 100 μL H_2O_2 (100 mM). The time-dependent change of UV–Vis absorbance at 652 nm was continuously recorded over 13 min at room temperature.

The effect of catalyst amount was screened on 2.6Pt/EMT from 0 to 1.0 mg under the same conditions. In a typical process, the peroxidase-mimicking reaction was performed at 298 K by using 0–1.0 mg of 2.6Pt/EMT catalyst in 3 mL of sodium acetate buffer (0.2 M, pH = 5.5) with 200 μL TMB (3 mM) and 100 μL H_2O_2 (100 mM). The time-dependent change of UV–Vis absorbance at 652 nm was continuously recorded over 13 min at room temperature.

The pH-dependent analysis was performed in different buffer solutions with pH ranging from 2.0 to 9.0, including glycine-HCl buffer (pH 2.0), sodium acetate buffer (pH 3.0–5.0), phosphate buffer (pH 6.0–8.0), carbonate buffer (pH 9.0). In a typical process, the peroxidase-mimicking reaction was performed at 298 K by using 0.45 mg of 2.6Pt/EMT catalyst in 3 mL buffer with 200 μL TMB (3 mM) and 100 μL H_2O_2 (100 mM). The time-dependent change of UV–Vis absorbance at 652 nm was continuously recorded over 13 min at room temperature.

The temperature-dependent study was carried out at the temperature ranging from 0 to 50 °C. In a typical process, the peroxidase-mimicking reaction was performed at 0–50 °C by using 0.45 mg of 2.6Pt/EMT catalyst in 3 mL of sodium acetate buffer (0.2 M, pH = 5.5) with 200 μL TMB (3 mM) and 100 μL H_2O_2 (100 mM). The time-dependent change of UV–Vis absorbance at 652 nm was continuously recorded over 13 min at different temperatures. The stability test was performed under normal conditions within one week. The conditions were the same as those described above, and catalyst stability was measured at room temperature.

Steady-state kinetic experiments were conducted with TMB as the substrate by using 0.45 mg of 2.6Pt/EMT catalyst in 3 mL sodium acetate buffer (pH = 5.5) with the same concentration of H_2O_2 (100 mM, 100 μL) and different concentrations of TMB (0.5, 1.0, 1.5, 2.0, 2.5, 3.0 mM, 200 μL). Similarly, the kinetic analysis with H_2O_2 as substrate was performed on 0.45 mg of 2.6Pt/EMT catalyst in 3 mL sodium acetate buffer (pH = 5.5), containing different concentrations of H_2O_2 (5.0, 10, 30, 50, 70, 100 mM, 100 μL) and fixed concentration of TMB (3.0 mM, 200 μL). The Michaelis-Menten equation (Formula (1)) was used to explain the catalytic behavior of 2.6Pt/EMT catalyst, where V_0 is the initial velocity, V_{max} is the maximum reaction velocity, [S] corresponds to the concentration of the substrate, and K_m is the Michaelis-Menten constant [42]. Then, the apparent kinetic parameters were calculated by using Lineweaver-Burk plots of the double reciprocal as Formula (2).

$$V_0 = \frac{V_{max}[S]}{K_m + [S]} \quad (1)$$

$$\frac{1}{V_0} = \frac{K_m}{V_{max}} \cdot \frac{1}{[S]} + \frac{1}{V_{max}} \quad (2)$$

2.5. Colorimetric detection of H_2O_2 and glucose

The limit of detection (LOD) of H_2O_2 was determined as follows: different concentrations of H_2O_2 (1.0–100 mM, 100 μL), 0.45 mg of 2.6Pt/EMT catalyst and 200 μL of TMB (3.0 mM) were added into 3 mL of sodium acetate buffer (0.2 M, pH = 5.5). Then, the absorbance of the mixed solution at 652 nm was measured after incubation for 13 min at room temperature.

The LOD of glucose was tested as follows. First, 200 μL of glucose solution with different concentrations (1.0–100 mM) was added into 1 mL of PBS (pH = 7.4), and after that 100 μL of GOx (2 mg/mL) was added into the above solution. After incubation at 310 K for 1.5 h, 0.45 mg of 2.6Pt/EMT catalyst, 200 μL of TMB (3.0 mM), and 3 mL of sodium acetate buffer (0.2 M, pH = 5.5) were successively added into the incubated glucose solution. After further reaction at 310 K for 1 h, the absorbance at 652 nm of the final mixture solution was measured at room temperature. In order to investigate the selectivity, the absorbance at 652 nm was compared for different solutions including 200 μL of 0.6 mM glucose, 6 mM fructose, 6 mM sucrose, and 6 mM lactose, respectively. Other conditions were the same as the above glucose measurement. The concentration of glucose in blood serum of diabetic patients was measured as follows. The serum of 100 μL was added into 1 mL of PBS (pH = 7.4) containing 100 μL of GOx (2 mg/mL), and then incubated at 310 K for 1 h. The subsequent incubation and determination steps were the same as that for glucose above. For the determination of glucose in various juices, the supernatant of peach juice and orange juice was first diluted in 250 folds for the experiment, respectively. And then the diluted solution of 100 μL was taken for analysis. The other conditions were the same with that for glucose determination above.

2.6. Characterizations

Powder X-ray diffraction (XRD) of the samples were measured on a Bruker D8 powder X-ray diffractometer (Bruker, Germany) using Cu K_α radiation (λ = 1.5406 Å) at 40 kV and 40 mA. The XRD patterns were taken in the angle range from 5 to 85°/2θ with a scan rate of 0.02°/min. Transmission electron microscopy (TEM) was performed by using a JEM 2011F microscope (JEOL, Japan) at 200 kV. Before determination, the samples were dispersed in absolute ethanol, and then the homogeneous suspension was dropped on Cu grids coated with holey carbon film. Scanning electron microscopy (SEM) images were taken on a field-emission microscope of S-4800 (Hitachi, Japan) operated at 1.0 kV. The Brunauer-Emmet-Teller (BET) surface area, pore volume and average pore size of samples were measured on a Quantachrome instrument (Quantachrome, USA) at liquid nitrogen temperature of 77 K. The samples were fully degassed in vacuum at 453 K overnight before measurement. X-ray photoelectron spectroscopy (XPS) was conducted on a Shimadzu/Kratos AXIS Ultra DLD spectrometer using Al K_α radiation as the excitation source. UV–Vis absorption spectra were recorded on a YOKE UV–Vis spectrophotometer (UV1900PC, China) using a 1 cm quartz cell. Scan Wavelength: 500.0–800.0 nm. Test Mode: Abs Mode.

3. Results and discussion

3.1. Structure characterizations

Fig. 1A shows XRD patterns of parent EMT zeolite and 2.6Pt/EMT nanocomposite, in which the diffraction peaks can be well assigned to the typical EMT zeolite [37]. The broadening of Bragg peaks in both samples is quite significant, suggesting that the synthesized EMT zeolite crystals are very small, and calculated by Scherrer Equation, the average particle size is about 13.8 nm. No diffraction peaks of metallic Pt in 2.6Pt/EMT nanocomposite (Fig. 1A-b, S1-a to c) appear in the pattern, indicating that Pt NPs are highly dispersed on the support of EMT zeolite. When Pt loading is actually up to 3.9 wt%, Pt NPs can be still highly dispersed without aggregation and breaking the zeolite framework (Fig. S1-d). The adsorption-desorption isotherms of the parent EMT zeolite and 2.6Pt/EMT nanocomposite are of the typical Type I, showing a rapid uptake at low relative pressure (P/P_0) and followed horizontal adsorption/desorption branches (Fig. 1B). This isotherm type is mainly attributed to the preferential filling of nitrogen molecules in zeolite micropores at lower P/P_0. The hysteresis loops at high P/P_0 demonstrate the presence of mesoporous structure in both samples, which stem from the accumulation of ultrasmall zeolite crystals. The BET surface area and total pore volume of parent EMT zeolite are as high as 522 m^2/g and 1.10 cm^3/g (Table 1), respectively, proving its high crystallinity with perfect microporous structure (micropore surface area = 302 m^2/g). High external

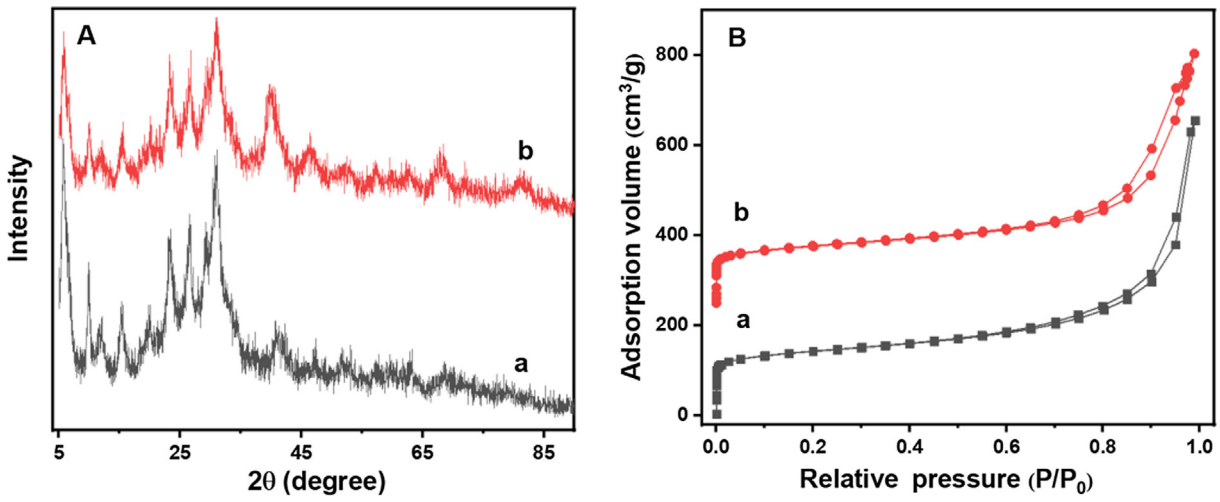

Fig. 1. XRD patterns (A), and nitrogen sorption isotherms (B) of parent EMT zeolite (a) and 2.6Pt/EMT nanocomposite (b), respectively (The sorption isotherms of 2.6Pt/EMT nanocomposite were vertically offset by 250 cm^3/g for clarity).

Table 1
Textural properties of the parent EMT zeolite and 2.6Pt/EMT nanocomposite.

Samples	BET surface area (m^2/g)	External surface area (m^2/g)	Micropore surface area (m^2/g)	Pore volume (cm^3/g)	Average pore size (nm)
EMT	522	220	302	1.10	7.7
2.6Pt/EMT	457	184	273	0.86	7.5

surface area of 220 m^2/g is mainly derived from the mesopores by stacking of the ultrasmall zeolite nanocrystals, and the average pore size is centered at 7.7 nm. After loading 2.6 wt% Pt NPs on EMT zeolite, BET surface area and total pore volume of the 2.6Pt/EMT nanocomposite slightly decrease to 457 m^2/g and 0.86 cm^3/g, respectively, which is mainly caused by the clogging and covering effect of Pt NPs onto partial micropores and zeolite external surface. Its micropore surface area remains as large as 273 m^2/g, demonstrating that Pt NPs are mainly decorated on the surface of ultrasmall EMT zeolite due to mismatch between the particle size of Pt NPs (5–8 nm) and the micropore size of EMT zeolite (0.71 nm), which can expose abundant catalytic interfaces for enzyme-mimicking catalysis.

Fig. 2 shows TEM images of the parent EMT zeolite and 2.6Pt/EMT nanocomposite. The EMT zeolite synthesized under mild conditions comprises a great number of uniform nanocrystals with slightly different morphology and average particle size of 15–20 nm (Fig. 2A and S2), in agreement with the result calculated by Scherrer Equation. The lattice fringes in hexagonal nanocrystals with d = 1.1 nm can be clearly observed (Fig. 2B), further demonstrating high crystallinity of the zeolite, which is quite consistent with its XRD result (Fig. 1A-a). The sample of 2.6Pt/EMT nanocomposite still retains the morphology and particle size of the parent EMT zeolite (Fig. 2C). Moreover, some highly-dispersed Pt NPs in size of 5–8 nm are confined within the zeolite (Fig. 2D), indicating that Pt NPs can be well decorated on the support of EMT zeolite crystals through impregnation of H_2PtCl_6 solution and $NaBH_4$ in situ reduction. When the solid powders of EMT and 2.6Pt/EMT were dispersed in water, the formed homogeneous suspension can be well stabilized without precipitation after a long period (Fig. S3), which showed the typical Tyndall effect under the radiation of laser beam (Fig. S4), proving the colloidal characteristics of the suspensions containing ultrasmall sized EMT and 2.6Pt/EMT NPs. Although no diffraction peaks about Pt NPs appear in the sample of 3.9Pt/EMT (Fig. S1-d), the dispersity of Pt NPs decreases with a certain aggregation into slightly larger particles (Fig. S5).

HRTEM image of 2.6Pt/EMT nanocomposite in Fig. 3A presents visible lattice fringes with d values of 0.227 and 0.254 nm, which are attributed to the [1 1 1] and [2 0 0] crystalline faces of Pt NPs, respectively. Fig. S6 also proves that highly-crystallized Pt NPs in average size of 5–8 nm are uniformly dispersed on the support of EMT zeolite. However, it's difficult to capture the lattice fringes of EMT zeolite, because it can be easily broken by electron beam when taking TEM images, indicating its weak stability caused by the ultrasmall particle size. To further characterize the valence state of surface Pt species loaded on EMT zeolite, XPS analysis was performed based on the sample of 2.6Pt/EMT nanocomposite (Fig. 3B). Since the silica-aluminum ratio of EMT zeolite is relatively low (Si/Al = 1.09), a kind of aluminum-riched zeolite, the binding energy peaks of Al_{2p} and Pt $4f_{5/2}$ are almost overlapped with each other, and the Al_{2p} peak should be separately fitted at 73.7 eV. The fitted peaks centered at 74.4 and 71.2 eV are attributed to metallic Pt (Pt^0 $4f_{7/2}$ and Pt^0 $4f_{5/2}$), and those at 74.9 and 72.1 eV are assigned to cationic Pt (Pt^{2+} $4f_{7/2}$ and Pt^{2+} $4f_{5/2}$) [41], indicating that metallic Pt and cationic Pt^{2+} species coexist in

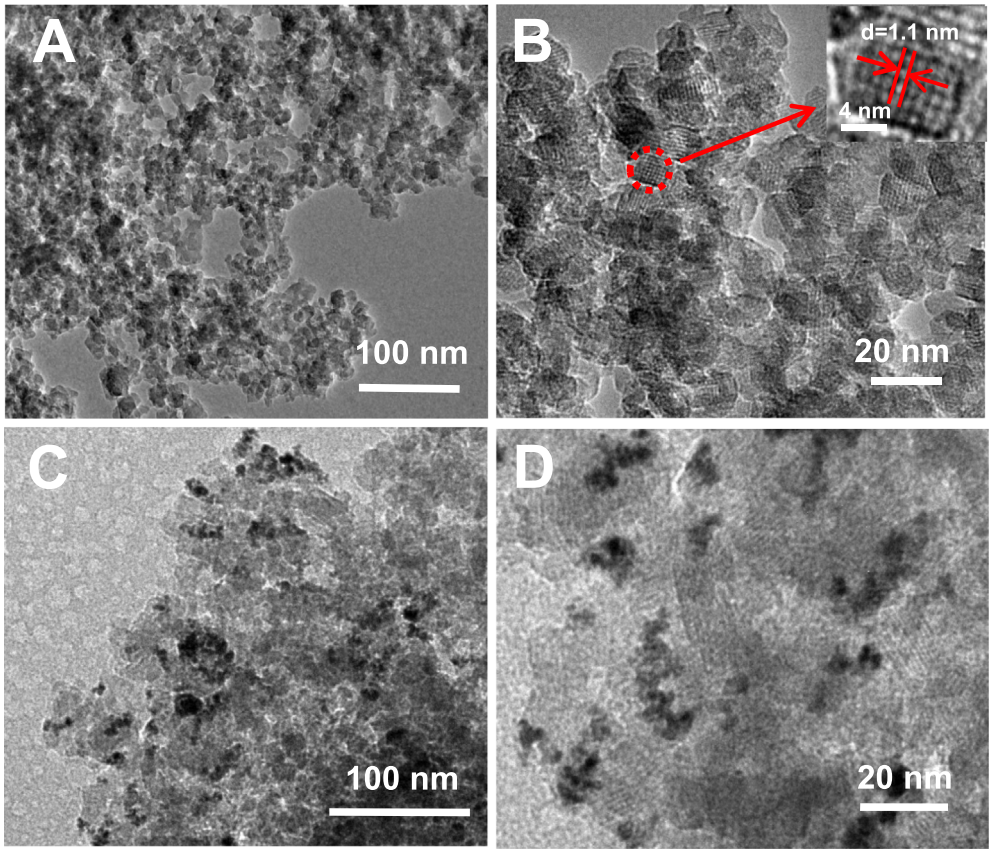

Fig. 2. TEM images of parent zeolite EMT (A, B) and 2.6Pt/EMT nanocomposite (C, D), respectively. The inset in the panel shows the crystalline lattice of zeolite.

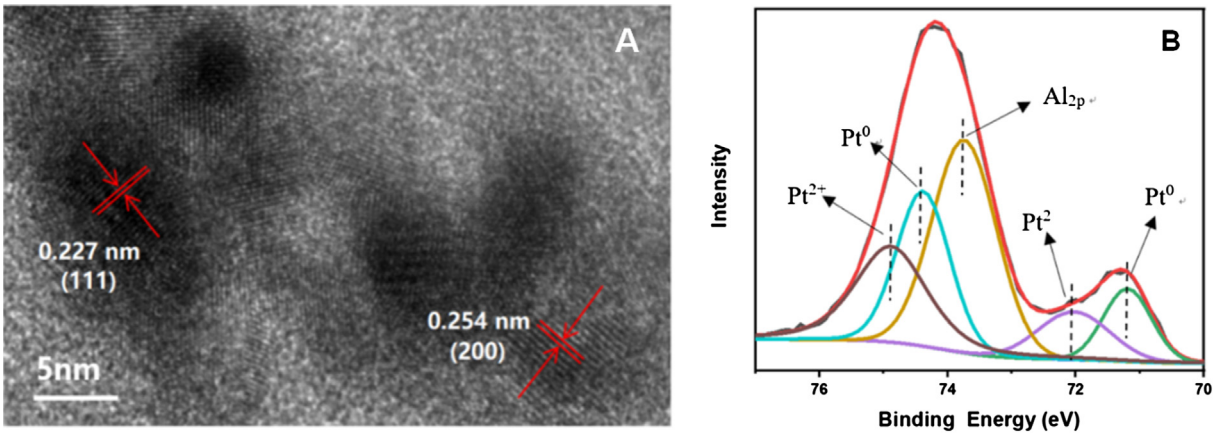

Fig. 3. (A) HRTEM image and (B) Pt_{4f} XPS spectrum of 2.6Pt/EMT nanocomposite.

Table 2
XPS analysis results of 2.6Pt/EMT nanocomposite.

Sample	Pt species	Peak area		Content (%)
		$Pt4f_{7/2}$	$Pt4f_{5/2}$	
2.6Pt/EMT	Pt^0	3121	7609	50.7%[a]
	Pt^{2+}	3039	7410	49.3%[b]

[a] Proportion of Pt^0 = Area (Pt^0)/ [Area (Pt^0) + Area (Pt^{2+})] × 100%.
[b] Proportion of Pt^{2+}=Area (Pt^{2+})/ [Area (Pt^0) + Area (Pt^{2+})] × 100%.

2.6Pt/EMT nanocomposite. By calculating the normalized peak areas, the content of metallic Pt^0 is about 50.7% (Table 2), slightly higher than that of cationic Pt^{2+}, both of which can perform as the active centers for peroxidase-like reactions [15].

3.2. Peroxidase-like activity of Pt/EMT nanocomposites

The peroxidase-like activity of Pt/EMT nanocomposite was evaluated toward TMB catalytic oxidation in the presence of H_2O_2, showing a visible color change by naked eyes, which was precisely monitored by UV–vis absorption spectroscopy at the wavelength of 652 nm. In the compared systems including H_2O_2, TMB, TMB + H_2O_2 and 2.6Pt/EMT + TMB, no color change happened with nearly no absorption at 652 nm in UV–vis spectra (Fig. 4A), demonstrating that the peroxidase-like reaction toward TMB as the substrate cannot perform spontaneously, or only by H_2O_2 or the catalyst of 2.6Pt/EMT. A strong absorption peak at 652 nm appears in the system of 2.6Pt/EMT + TMB + H_2O_2 under the same conditions, indicating that TMB was oxidized into ox-TMB after the addition of 2.6Pt/EMT nanocomposite in the presence of H_2O_2, which confirms its good peroxidase-like activity. In fact, the support of EMT zeolite itself shows almost no catalytic activity (Fig. 4B), proving that the Pt species perform as the active sites for peroxidase-like reactions. The commercial zeolite Y (Fig. S7) with slightly higher Si/Al ratio of about 1.5 and larger particle size of 500 nm was used as the support to load 2.6 wt% Pt for comparison. The activity of the obtained 2.6Pt/Y nanocomposite is only 21% based on 100% catalytic activity of 2.6Pt/EMT. Although zeolite Y has the similar microporous structure with EMT, its higher Si/Al ratio and larger particle size result in lower peroxidase-like activity of 2.6Pt/Y. The results prove that ultrasmall EMT zeolite is a superior support, which can uniformly load Pt NPs in size of 5–8 nm on its surface to form the active enzyme-mimicking catalyst. As discussed above, Pt species are the active sites for peroxidase-like reactions, so the catalytic efficiency is primarily affected by the amounts of Pt species through changing the Pt to EMT mass ratios and the mass of used catalyst in the system (Fig. 5). The catalytic activity toward TMB

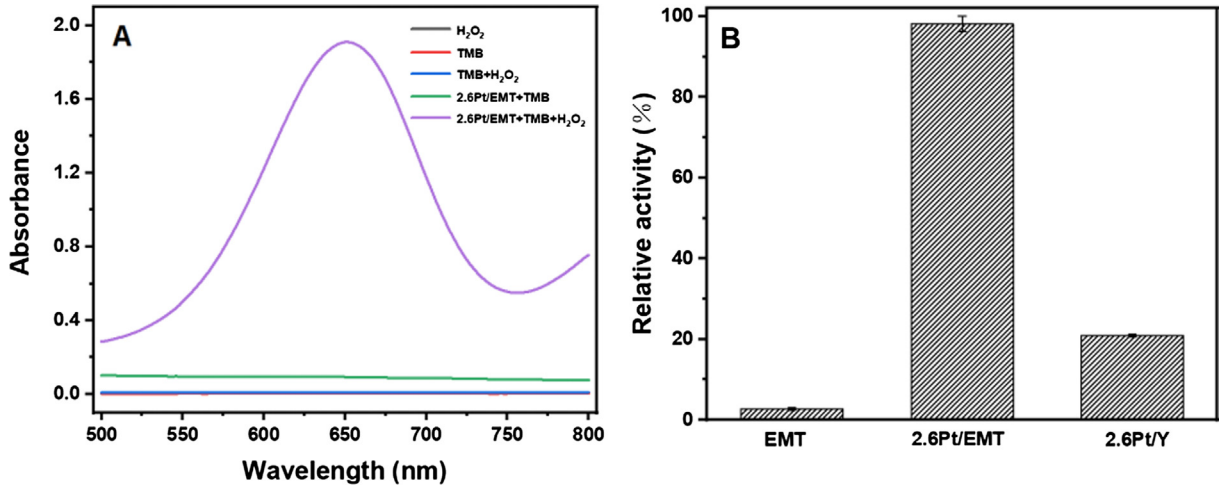

Fig. 4. (A) Typical absorption spectra of TMB-H_2O_2 solution in the absence and presence of 2.6Pt/EMT nanocomposite catalyst: H_2O_2, TMB, TMB + H_2O_2, TMB + 2.6Pt/EMT, and TMB + H_2O_2 + 2.6Pt/EMT. (B) Relative activity of different catalysts including parent zeolite EMT, 2.6Pt/EMT nanocomposite and 2.6Pt/Y nanocomposite. Experimental conditions: catalysts: 0.45 mg; acetate buffer: 0.2 M (pH = 5.5); TMB: 3 mM; H_2O_2: 100 mM; the reaction mixture was incubated at 25 °C for 13 min, and the absorbance was measured at room temperature.

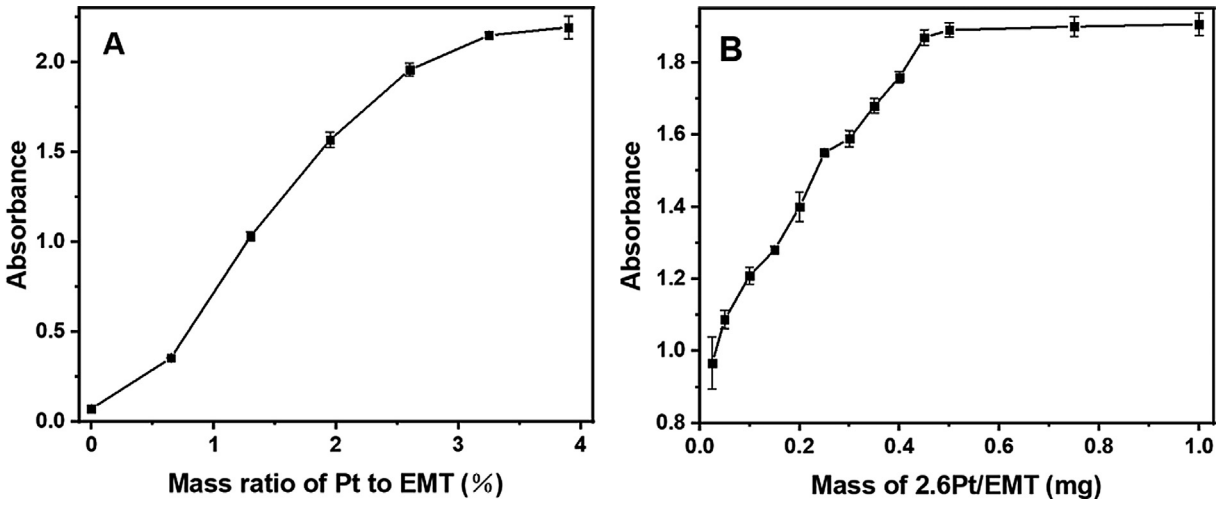

Fig. 5. (A) Variations of catalytic activity of *x*Pt/EMT nanocomposites with *x* from 0 to 3.9 (catalyst: 0.45 mg), and (B) mass effects of the added 2.6Pt/EMT nanocomposite in the system from 0 to 1.0 mg. Experimental conditions: acetate buffer: 0.2 M (pH = 5.5); TMB: 3 mM; H_2O_2: 100 mM; the reaction mixtures were incubated at 25 °C for 13 min, and the absorbance was measured at room temperature.

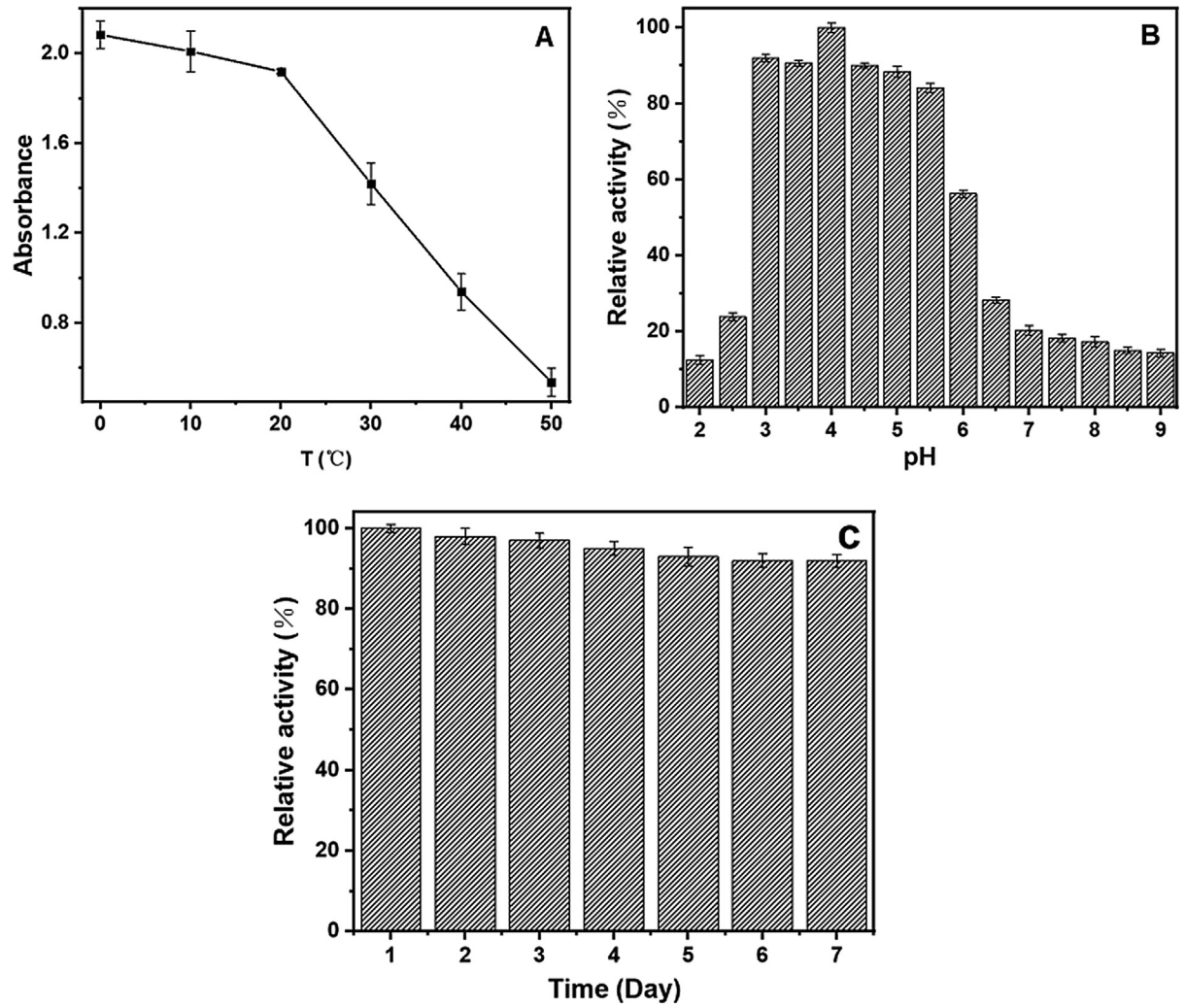

Fig. 6. The optimization of incubation temperature (A) and pH (B) for the catalytic activity of 2.6Pt/EMT nanocomposite. (C) Environmental catalytic stability test of 2.6Pt/EMT nanocomposite within one week. Experimental conditions: catalysts: 0.45 mg; TMB: 3 mM; H_2O_2: 100 mM, the absorbance was measured at room temperature after incubation.

oxidation increases almost linearly as the mass ratio of Pt to EMT increases from 0.65 wt% to 2.6 wt% (Fig. 5A), demonstrating a gradual increase of active centers exposed on the surface of ultrasmall EMT zeolite up to the Pt loading threshold of 2.6 wt%. Over this point the activity toward TMB oxidation has a slow increase until to 3.9 wt% of Pt loading, mainly because of the aggregation of excess Pt NPs on EMT zeolite, which have almost no contribution to enhancement of peroxidase-like activity. Therefore, the sample of 2.6Pt/EMT was considered as the optimal catalyst in this work. Fig. 5B presents the variations of catalytic activity with mass of 2.6Pt/EMT nanocomposite in the system. The absorbance at 652 nm increases nearly linearly from 0.025 mg to 0.45 mg of catalysts, and then remains unchanged from 0.45 mg to 1.0 mg. Therefore, 0.45 mg of 2.6Pt/EMT catalyst is the most suitable amount in this fixed TMB-H_2O_2 system.

Similar with the natural enzyme HRP and other peroxidase mimics, the catalytic activity of Pt/EMT nanocomposites is also dependent on the reaction conditions including incubation temperature and pH values. Herein, the peroxidase-like activity of 2.6Pt/EMT was screened in the system by changing the temperature from 0 to 50 °C and pH values from 1.0 to 9.0. It's well accepted that the activity of peroxidase catalysts is greatly affected by reaction temperatures, and generally the natural enzyme of HRP can only performs high efficiency within a narrow temperature range (20–30 °C) [5]. It can be seen from Fig. 6A that the catalytic activity of 2.6Pt/EMT nanocomposite slightly decreases with the

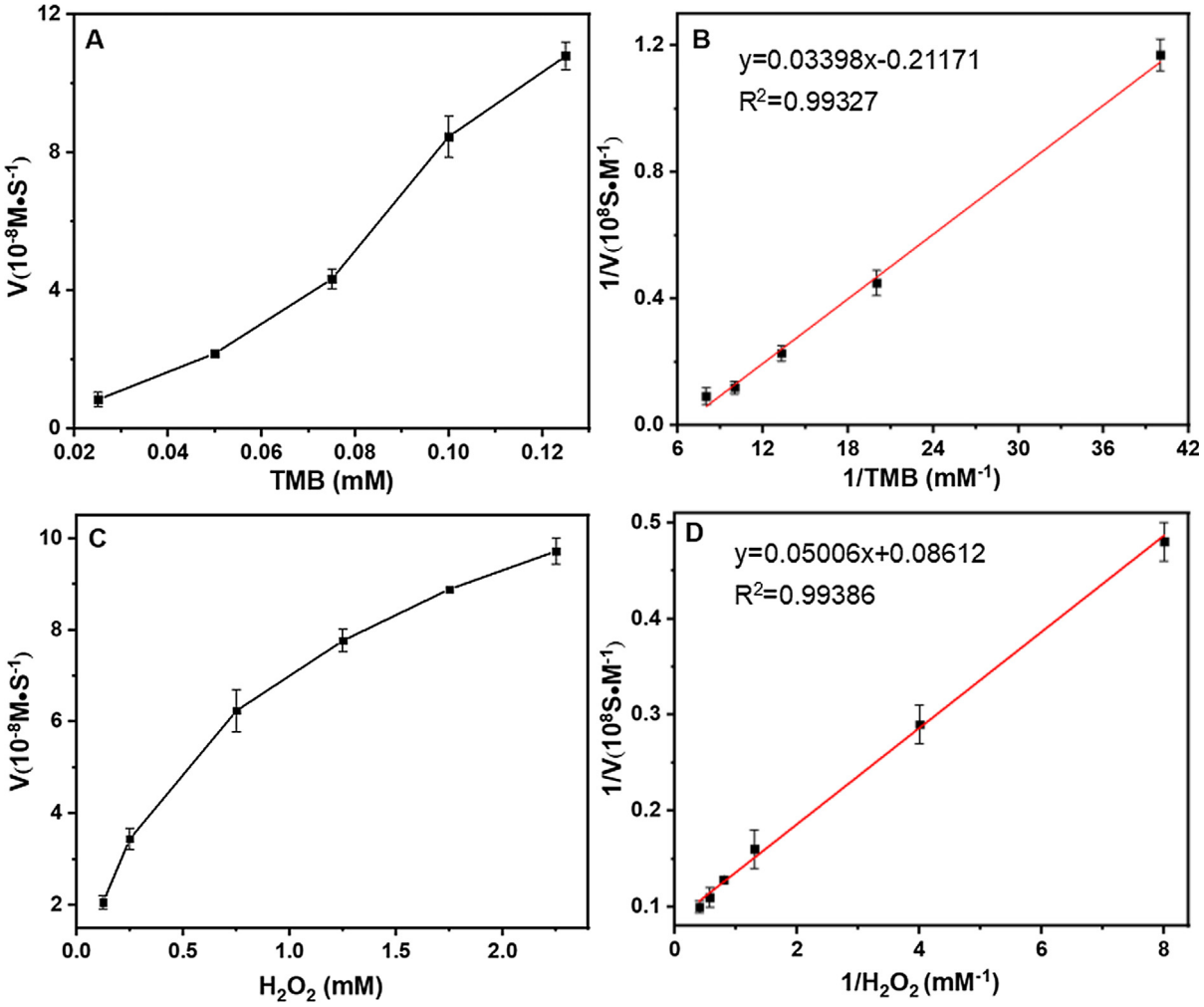

Fig. 7. The steady-state kinetic analysis based on Michaelis-Menten model (A, C) and Lineweaver-Burk double-reciprocal model (B, D) for the catalyst of 2.6Pt/EMT nanocomposite, respectively. The concentration of H_2O_2 was fixed at 100 mM while TMB concentration was altered from 0.5 mM to 3 mM (A, B). The concentration of TMB was fixed at 3 mM and H_2O_2 concentration was varied from 5 mM to 100 mM. Other experimental conditions: catalysts: 0.45 mg; acetate buffer: 0.2 M (pH = 5.5); the reaction mixtures were incubated at 25 °C for 13 min, and the absorbance was measured at room temperature.

Table 3
Comparison of the apparent Michaelis-Menten constant (K_m) and the maximum reaction rate (V_{max}) calculated from the double reciprocal plots.

Substrate	Catalyst	K_m (mM)	V_{max} (10^{-8} M S^{-1})	k_{cat} (min^{-1})
TMB	2.6Pt/EMT	0.16	4.72	17.7
TMB	HRP[#]	0.43	10.0	14.0
H_2O_2	2.6Pt/EMT	0.58	11.6	12.0
H_2O_2	HRP[#]	3.73	8.71	1.40

[#] The data of K_m and V_{max} for HRP are from the literature [5].

increasing of temperatures from 0 to 20 °C, indicating a good low-temperature activity and stability as a peroxidase-like catalyst. The absorbance at 652 nm decreases with the increasing of temperature from 20 to 50 °C, showing a quite different catalytic performance from CeO_2/Y nanocomposite and other peroxidase-like catalysts, whose activity generally increased as the temperature increasing from 15 to 65 °C [38]. This result illustrates that the 2.6Pt/EMT nanocomposite is adapted to peroxidase-like reactions at relatively low temperatures even close to 0 °C, which is mainly due to low stability of Pt/EMT nanocomposite at the temperature higher than 30 °C [36]. When pH values increase from 2.0 to 4.0, the relative activity of 2.6Pt/EMT nanocomposite quickly increases from 12.5% to 100%, and then it gradually decreases in the pH range of 4.0–6.5 (Fig. 6B). The catalyst shows relative low activity under alkaline (pH > 7) and strong acidic (pH < 3) conditions, due to the instability of EMT zeolite support and active sites of Pt NPs. Therefore, the optimal pH is in the weakly acidic range of 3.0–5.5, which facilitates the formation of peroxide species on catalytic centers of Pt NPs and then quick oxidation of TMB into ox-TMB. Finally, the long-term stability of 2.6Pt/EMT nanocomposite was tested within one weak (Fig. 6C), showing no significant decrease of catalytic activity in each day. After 7-days storage at room temperature, the relative activity of 2.6Pt/EMT nanocomposite can still reach up to 90%, indicating its outstanding stability as a peroxidase-like catalyst.

3.3. Kinetic studies of peroxidase-like activity of 2.6Pt/EMT nanocomposite

Based on the steady-state kinetics theory and methods, the peroxidase-like catalytic performance of 2.6Pt/EMT nanocomposite toward H_2O_2 and TMB as substrates was investigated in detail, both of which display the typical Michaelis-Menten curves within a suitable concentration range (Fig. 7A and C). The apparent steady-state kinetic parameters, including the Michaelis-Menten constant (K_m) and the maximum velocity (V_{max}), can be calculated by the linear fitting from the Lineweaver-Burk double-reciprocal plots (Fig. 7B and D) [42]. The K_m value indicates the affinity of substrate (TMB and H_2O_2) to catalyst, and a lower K_m value reflects a stronger affinity. As shown in Table 3, the K_m values of 2.6Pt/EMT nanocomposite toward H_2O_2 and TMB are 0.16 mM and 0.58 mM, respectively, which are much smaller than those of the natural

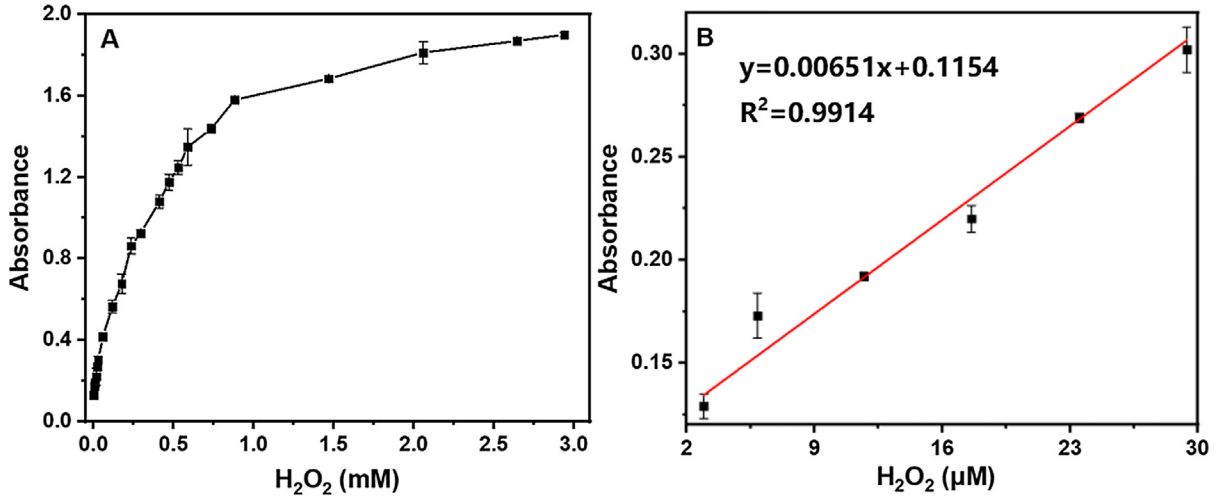

Fig. 8. (A) The H_2O_2 concentration response curve using the catalyst of 2.6Pt/EMT nanocomposite, and (B) the corresponding linear calibration plot for H_2O_2 in the range of 2.9–29.4 μM. Experimental conditions: catalysts: 0.45 mg; TMB: 3 mM; acetate buffer: 0.2 M (pH = 5.5); the reaction mixtures were incubated at 25 °C for 13 min, and the absorbance was measured at room temperature.

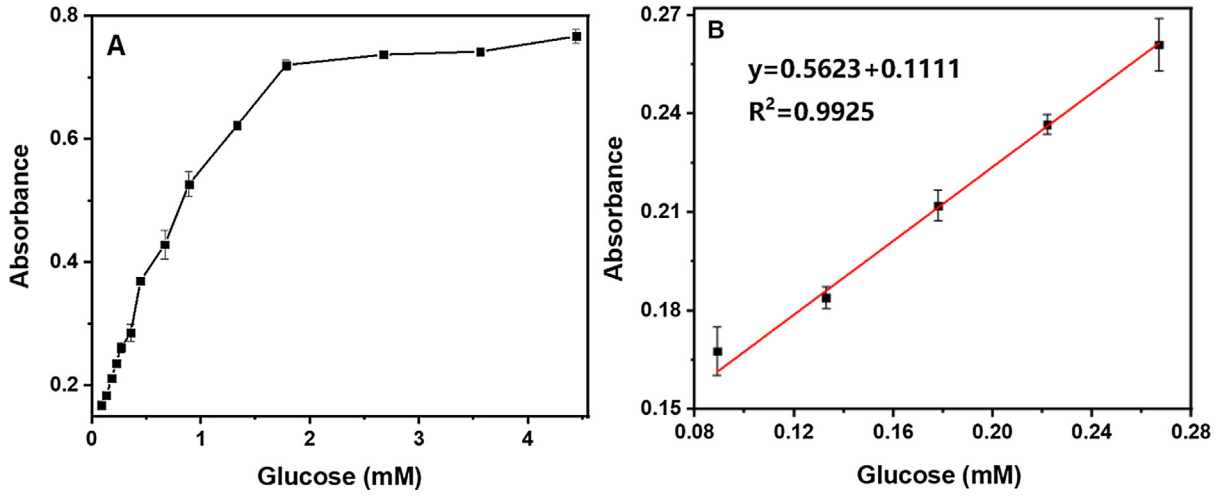

Fig. 9. (A) The glucose concentration response curve using the catalyst of 2.6Pt/EMT nanocomposite, and (B) the corresponding linear calibration plot for glucose in the range of 0.09–0.27 mM. Experimental conditions: catalysts: 0.45 mg; acetate buffer: 0.2 M (pH = 5.5); PBS buffer (pH = 7.4); TMB: 3 mM; the reaction mixtures were incubated at 25 °C for 13 min, and the absorbance was measured at room temperature.

enzyme HRP, suggesting that the peroxidase mimic of 2.6Pt/EMT has higher affinity for both substrates, therefore, TMB and H_2O_2 with lower concentration are needed for 2.6Pt/EMT than that for HRP to reach the maximum activity, mainly due to its porous structure, ultrasmall particle size and highly dispersed Pt NPs. Moreover, the V_{max} value of 2.6Pt/EMT toward H_2O_2 is slightly higher than that of HRP (Table 3), declaring its promising peroxidase-like activity. Furthermore, the higher derived catalytic constant (k_{cat}) of 2.6Pt/EMT toward H_2O_2 (12.0 min^{-1}) is 8.56 times towards HRP, indicating its excellent catalytic efficiency as a peroxidase-mimicking catalyst.

3.4. Detection of H_2O_2 and glucose by using 2.6Pt/EMT nanocomposite

H_2O_2 and glucose are widely used in identification of biomedical and food research, therefore, it is of importance to precisely determine their concentration in the complex systems. Since the catalyst of 2.6Pt/EMT nanocomposite exhibits the excellent performance as a peroxidase mimic in determination of H_2O_2 and glucose, here a facile colorimetric method was conducted to rapidly determine H_2O_2 and glucose concentration. As shown in Fig. 8A, the absorbance of the systems gradually increases as H_2O_2 concentration increasing from 0 to 3.0 mM under the same conditions. A good linear relationship (R^2 = 0.9914) is presented between the absorbance of ox-TMB and H_2O_2 in the concentration range of 2.9–29.4 μM (Fig. 8B), and the LOD of H_2O_2 is calculated to be about 1.1 μM, comparable to the results in previous report (Table S1). For glucose detection, it was firstly transformed into H_2O_2 and gluconic acid through oxidation reaction by glucose oxidase (GOx), and then the produced H_2O_2 was detected by the colorimetric method based on TMB oxidation under the catalytic effect of 2.6Pt/EMT nanocomposite, which were well related to the concentration of glucose in solution. The absorbance of the solution gradually increases with glucose concentration from 0 to 2 mM (Fig. 9A), and a significant linear correlation is illustrated for the glucose concentration response curve in a concentration range of 0.09–0.27 mM (Fig. 9B). The LOD of glucose on 2.6Pt/EMT nanocomposite was calculated to be around 13.2 μM, which is comparable to the results in previous report (Table S1). The selectivity to glucose against other sugars on the catalyst of 2.6Pt/EMT nanocomposite is shown in Fig. 10, which is a key factor to evaluate whether the peroxidase mimic can be used in the complex systems. Because the enzyme of GOx has a high specificity toward glucose, the response of the 2.6Pt/EMT nanocomposite is very weak to the contrast sugars including fructose, lactose and sucrose even with high concentrations of 10 times glucose, indicating a high selectivity for glucose based on the peroxidase-like catalyst of 2.6Pt/EMT. By using this colorimetric method, the concentration of glucose in real samples such as human blood serum and fruit juices (peach juice and orange juice) was measured (Fig. 11). According to the calibration curve of absorbance to glucose concentration in Fig. 9B, the concentration of glucose in the serum sample of a diabetic is calculated to be about 10.1 mM, which is quite consistent with the given concentration of 10.7 mM determined by a spectrophotometric method. Furthermore, using this method we can detect the concentration of glucose in different juices, such as peach juice (0.78 M) and orange juice (0.71 M), further proving high reliability of the colorimetric method by using the peroxidase mimic of 2.6Pt/EMT to determine the glucose concentration in real samples.

The outstanding performance of 2.6Pt/EMT nanocomposite as the peroxidase mimic has a close relationship with its intrinsic structures. Firstly, the three-dimensional pore structure with 12-membered ring micropores of the EMT zeolite facilitates the diffusion of hydrogen peroxide and TMB inside the material, thereby improving the catalytic efficiency. In addition, the ultrasmall EMT zeolite has huge external surface for homogeneous and stable dispersion of Pt NPs through a strong interfacial interaction, and the hybrid Pt/EMT nanomaterials exhibit highly exposed surface and abundant catalytic interface. The much shorter diffusion distance also endows the material with accessible active sites, which further enhance the catalytic performance. The highly-dispersed Pt NPs in size of 5–8 nm is favorable for H_2O_2 decomposition and TMB oxidation, due to the facile transformation of Pt^0 and Pt^{2+}. Besides, the EMT zeolite support possesses large micropore surface area and micropore volume, which can greatly strengthen the adsorption of TMB and H_2O_2 on the catalyst surface.

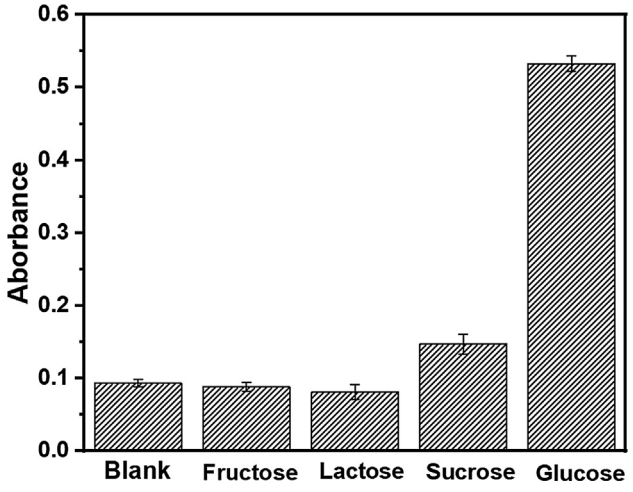

Fig. 10. The selectivity of glucose detection with different sugars (6 mM fructose, 6 mM sucrose, 6 mM lactose, and 0.6 mM glucose) after incubation in the system containing glucose oxidase and 2.6Pt/EMT nanocomposite. Experimental conditions: catalysts: 0.45 mg; acetate buffer: 0.2 M (pH = 5.5); PBS buffer (pH = 7.4); TMB: 3 mM; the reaction mixtures were incubated at 25 °C for 13 min, and the absorbance was measured at room temperature.

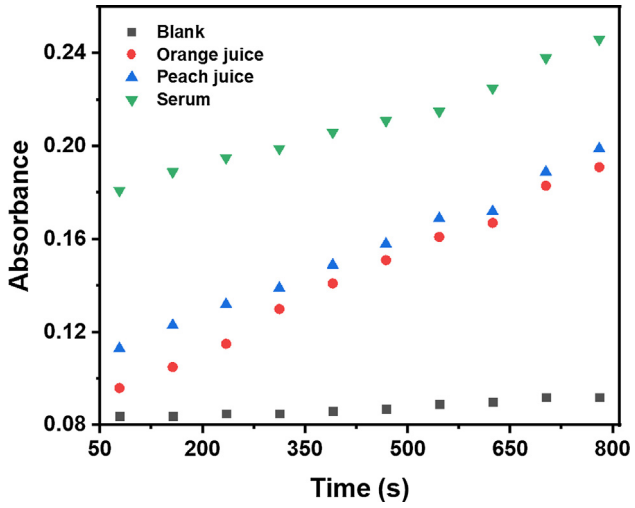

Fig. 11. The time-dependent absorbance changes at 652 nm for different samples (water, diluted orange juice, diluted peach juice, and human serum samples) after incubation in the system containing glucose oxidase and 2.6Pt/EMT nanocomposite. Fruit juice was diluted in 250 folds, and no dilution treatment was conducted for the blood sample. Experimental conditions: catalysts: 0.45 mg; acetate buffer: 0.2 M (pH = 5.5); PBS buffer (pH = 7.4); TMB: 3 mM; the reaction mixtures were incubated at 25 °C for 13 min, and the absorbance was measured at room temperature.

4. Conclusions

In summary, we developed a novel colorimetric method for H_2O_2 and glucose detection by using Pt NPs loaded on ultrasmall EMT zeolite as peroxidase mimics. The ultrasmall EMT zeolite in size of 15–20 nm was synthesized in a template-free colloidal system by a low-temperature crystallization method, which was used as a support for high dispersion of Pt NPs (5–8 nm) onto its surface through a facile wet impregnation and $NaBH_4$ in situ reduction strategy. The Pt/EMT nanocomposites showed large surface area (457 m^2/g) and pore volume (0.86 cm^3/g), and ultrasmall particle size (15–20 nm), which could be dispersed in water to form homogeneous suspension. The activity of Pt/EMT peroxidase-like catalyst is dependent on Pt NPs content (Pt to EMT ratio), catalyst amount, pH value, incubation temperature, H_2O_2 and TMB concentration. The optimal catalyst of 2.6Pt/EMT nanocomposite showed higher affinity to H_2O_2 and TMB than HRP through steady-state kinetic analysis, allowing the measurement of H_2O_2 concentration within the linear range of 2.9–29.4 μM, with a limit of detection as low as 1.1 μM. In addition, the colorimetric method could be used to measure glucose concentration with a low limit of detection of 13.2 μM and a wide linear range (0.09–0.27 mM). More importantly, due to high selectivity to glucose against other sugars, the 2.6Pt/EMT nanocomposite could be used as the peroxidase-like catalyst in accurate detection of glucose in real blood serum samples and fruit juices, suggesting its great potential in clinical diagnosis, food detection, biochemical analysis, and so on.

CRediT authorship contribution statement

Xiaolong Li: Conceptualization, Methodology, Writing - original draft. **Xuanyu Yang:** Data curation, Writing - review & editing. **Xiaowei Cheng:** Conceptualization, Methodology, Writing - review & editing, Supervision. **Yuye Zhao:** Investigation. **Wei Luo:** Resources, Investigation. **Ahmed A. Elzatahry:** Visualization, Formal analysis. **Abdulaziz Alghamdi:** Visualization. **Xing He:** Visualization. **Jiacan Su:** Visualization. **Yonghui Deng:** Supervision.

Declaration of Competing Interest

None.

Acknowledgments

This work was supported by Key Basic Research Program of Science and Technology Commission of Shanghai Municipality (17JC1400100), the NSF of China (21673048, 21875044, 51822202 and 51772050), Program of Shanghai Academic Research Leader (19XD1420300), Shanghai Rising-Star Program (18QA1400100), the state key laboratory of Transducer Technology of China (SKT1904) and National Youth Topnotch Talent Support Program of China. The authors would like extend their thanks to the project (RSP-2019/155) by King Saud University, Riyadh, Saudi Arabia.

Appendix A. Supplementary material

Supplementary data to this article can be found online at https://doi.org/10.1016/j.jcis.2020.02.118.

References

[1] L. Gao, J. Zhuang, L. Nie, J. Zhang, Y. Zhang, N. Gu, T. Wang, J. Feng, D. Yang, S. Perrett, X. Yan, Intrinsic peroxidase-like activity of ferromagnetic nanoparticles, Nat. Nanotech. 2 (2007) 577–583.
[2] Y. Lin, J. Ren, X. Qu, Catalytically active nanomaterials: a promising candidate for artificial enzymes, Acc. Chem. Res. 47 (2014) 1097–1105.
[3] L. Artiglia, S. Agnoli, M.C. Paganini, M. Cattelan, G. Granozzi, TiO_2@CeO_x core-shell nanoparticles as artificial enzymes with peroxidase-like activity, ACS Appl. Mater. Interfaces. 6 (2014) 20130–20136.
[4] X. Ren, M. Wang, X. He, Z. Li, J. Zhang, W. Zhang, X. Chen, H. Ren, X. Meng, Superoxide dismutase mimetic ability of Mn-doped ZnS QDs, Chin. Chem. Lett. 29 (2018) 1865–1868.
[5] X. Yang, P. Qiu, J. Yang, Y. Fan, L. Wang, W. Jiang, X. Cheng, Y. Deng, W. Luo, Mesoporous materials–based electrochemical biosensors from enzymatic to nonenzymatic, Small 1904022 (2019).
[6] R. André, F. Natálio, M. Humanes, J. Leppin, K. Heinze, R. Wever, H.C. Schröder, W.E.G. Müller, W. Tremel, V_2O_5 Nanowires with an intrinsic peroxidase-like activity, Adv. Funct. Mater. 21 (2011) 501–509.
[7] J. Ge, X. Yang, J. Luo, J. Ma, Y. Zou, J. Li, W. Luo, X. Cheng, Y. Deng, Ordered mesoporous CoO/CeO_2 heterostructures with highly crystallized walls and enhanced peroxidase-like bioactivity, Appl. Mater. Today. 15 (2019) 482–493.
[8] M. Zhang, L. Xu, Q. Ma, H. Yu, H. Fang, Z. Lin, Q. Zhang, Z. Chen, A pH-controlled kit for total and direct bilirubin built on mimetic peroxidase $CoFe_2O_4$-DOPA-catalyzed fluorescence enhancement, ACS Appl. Mater. Interfaces 10 (2018) 42155–42164.
[9] H. Chen, Y. Li, F. Zhang, G. Zhang, X. Fan, Graphene supported Au-Pd bimetallic nanoparticles with core-shell structures and superior peroxidase-like activities, J. Mater. Chem. 21 (2011) 17658–17661.
[10] C.M. Cova, A. Zuliani, M.J. Muñoz-Batista, R. Luque, A Sustainable approach for the synthesis of catalytically active peroxidase-mimic ZnS catalysts, ACS Sustain. Chem. Eng. 7 (2019) 1300–1307.
[11] C. Guo, Y. Jiao, Y. Zheng, J. Luo, K. Davey, S. Qiao, Intermediate modulation on noble metal hybridized to 2D metal-organic framework for accelerated water electrocatalysis, Chem. 5 (2019) 2429–2441.
[12] L. Jin, Z. Meng, Y. Zhang, S. Cai, Z. Zhang, C. Li, L. Shang, Y. Shen, Ultrasmall Pt nanoclusters as robust peroxidase mimics for colorimetric detection of glucose in human serum, ACS Appl. Mater. Interfaces 9 (2017) 10027–10033.
[13] K. Cai, Z. Lv, K. Chen, L. Huang, J. Wang, F. Shao, Y. Wang, H. Han, Aqueous synthesis of porous platinum nanotubes at room temperature and their intrinsic peroxidase-like activity, Chem. Commu. 49 (2013) 6024–6026.
[14] M. Ma, Y. Zhang, N. Gu, Peroxidase-like catalytic activity of cubic Pt nanocrystals, Colloid Surf. A 373 (2011) 6–10.
[15] Z. Gao, M. Xu, L. Hou, G. Chen, D. Tang, Irregular-shaped platinum nanoparticles as peroxidase mimics for highly efficient colorimetric immunoassay, Anal. Chim. Acta 776 (2013) 79–86.
[16] X. Liu, X. Wang, Q. Han, W. Xiao, S. Cai, W. Wang, Sensitive colorimetric detection of ascorbic acid using Pt/CeO_2 nanocomposites as peroxidase mimics, Appl. Surf. Sci. 479 (2019) 532–539.
[17] X. Hu, A. Saran, S. Hou, T. Wen, Y. Ji, W. Liu, H. Zhang, W. He, J.J. Yin, X. Wu, Au@PtAg core/shell nanorods: tailoring enzyme-like activities via alloying, RSC Adv. 3 (2013) 6095–6105.
[18] X. Sun, S. Guo, Y. Liu, S. Sun, Dumbbell-like PtPd-Fe_3O_4 nanoparticles for enhanced electrochemical detection of H_2O_2, Nano Lett. 12 (2012) 4859–4863.
[19] J. Fan, J.J. Yin, B. Ning, X. Wu, Y. Hu, M. Ferrari, G.J. Anderson, J. Wei, Y. Zhao, G. Nie, Direct evidence for catalase and peroxidase activities of ferritin-platinum nanoparticles, Biomaterials 32 (2011) 1611–1618.
[20] Y. Ju, J. Kim, Dendrimer-encapsulated Pt nanoparticles with peroxidase-mimetic activity as biocatalytic labels for sensitive colorimetric analyses, Chem. Commu. 51 (2015) 13752–13755.
[21] Z. Wang, X. Yang, J. Yang, Y. Jiang, N. He, Peroxidase-like activity of mesoporous silica encapsulated Pt nanoparticle and its application in colorimetric immunoassay, Anal. Chim. Acta 862 (2015) 53–63.
[22] D. Jo, G.T. Park, T. Ryu, S.B. Hong, Economical synthesis of high-silica LTA zeolites: A step forward in developing a new commercial NH_3-SCR catalyst, Appl. Catal., B: Environ. 243 (2019) 212–219.
[23] X. Liu, M. Wang, C. Zhou, W. Zhou, K. Cheng, J. Kang, Q. Zhang, W. Deng, Y. Wang, Selective transformation of carbon dioxide into lower olefins with a bifunctional catalyst composed of $ZnGa_2O_4$ and SAPO-34, Chem. Commu. 54 (2018) 140–143.
[24] Z. Jin, L. Wang, Q. Hu, L. Zhang, S. Xu, X. Dong, X. Gao, R. Ma, X. Meng, F.-S. Xiao, Hydrophobic zeolite containing titania particles as wettability-selective catalyst for formaldehyde removal, ACS Catal. 8 (2018) 5250–5254.
[25] C. Wang, Z. Liu, L. Wang, X. Dong, J. Zhang, G. Wang, S. Han, X. Meng, A. Zheng, F.-S. Xiao, Importance of zeolite wettability for selective hydrogenation of furfural over Pd@zeolite catalysts, ACS Catal. 8 (2017) 474–481.
[26] S. Shwan, M. Skoglundh, L.F. Lundegaard, R.R. Tiruvalam, T.V.W. Janssens, A. Carlsson, P.N.R. Vennestrøm, Solid-state ion-exchange of copper into zeolites facilitated by ammonia at low temperature, ACS Catal. 5 (2014) 16–19.
[27] J. Rui, J. Lyu, H. Hu, Q. Zhang, Q. Wang, X. Li, Synthesized high-silica hierarchical porous ZSM-5 and optimization of its reaction conditions in benzene alkylation with methanol, Chin. Chem. Lett. 30 (2019) 757–761.
[28] Y. Guo, T. Sun, X. Liu, Q. Ke, X. Wei, Y. Gu, S. Wang, Cost-effective synthesis of CHA zeolites with controllable morphology and size, Chem. Eng. J. 358 (2019) 331–339.
[29] N. Zhu, Z. Lian, Y. Zhang, W. Shan, H. He, Improvement of low-temperature catalytic activity over hierarchical Fe-Beta catalysts for selective catalytic reduction of NO with NH_3, Chin. Chem. Lett. 30 (2019) 867–870.
[30] J. Jin, C. Peng, J. Wang, H. Liu, X. Gao, H. Liu, C. Xu, Facile synthesis of mesoporous zeolite Y with improved catalytic performance for heavy oil fluid catalytic cracking, Ind. Eng. Chem. Res. 53 (2014) 3406–3411.

[31] R.J. White, A. Fischer, C. Goebel, A. Thomas, A sustainable template for mesoporous zeolite synthesis, J. Am. Chem. Soc. 136 (2014) 2715–2718.
[32] X. Zhou, Y. Chen, T. Ge, Z. Hua, H. Chen, J. Shi, Sodium carbonate-assisted synthesis of hierarchically porous single-crystalline nanosized zeolites, Sci. Bull. 62 (2017) 1018–1024.
[33] T. Wakihara, R. Ichikawa, J. Tatami, A. Endo, K. Yoshida, Y. Sasaki, K. Komeya, T. Meguro, Bead-milling and postmilling recrystallization: an organic template-free methodology for the production of nano-zeolites, Cryst. Growth Des. 11 (2011) 955–958.
[34] M. Dusselier, M.E. Davis, Small-Pore zeolites: synthesis and catalysis, Chem. Rev. 118 (2018) 5265–5329.
[35] H. Awala, J.P. Gilson, R. Retoux, P. Boullay, J.M. Goupil, V. Valtchev, S. Mintova, Template-free nanosized faujasite-type zeolites, Nat. Mater. 14 (2015) 447–451.
[36] E.-P. Ng, J.-M. Goupil, A. Vicente, C. Fernandez, R. Retoux, V. Valtchev, S. Mintova, Nucleation and crystal growth features of EMT-Type zeolite synthesized from an organic-template-free system, Chem. Mater. 24 (2012) 4758–4765.
[37] E.P. Ng, D. Chateigner, T. Bein, V. Valtchev, S. Mintova, Capturing ultrasmall EMT zeolite from template-free systems, Science 335 (2012) 70–73.
[38] B. Dong, S. Belkhair, M. Zaarour, L. Fisher, J. Verran, L. Tosheva, R. Retoux, J.P. Gilson, S. Mintova, Silver confined within zeolite EMT nanoparticles: preparation and antibacterial properties, Nanoscale 6 (2014) 10859–10864.
[39] X. Cheng, L. Huang, X. Yang, A.A. Elzatahry, A. Alghamdi, Y. Deng, Rational design of a stable peroxidase mimic for colorimetric detection of H_2O_2 and glucose: a synergistic CeO_2/Zeolite Y nanocomposite, J. Colloid Interface Sci. 535 (2019) 425–435.
[40] Y. Fan, Z. Yang, P. Huang, X. Zhang, Y. Liu, Pt/TiO_2-C with hetero interfaces as enhanced catalyst for methanol electrooxidation, Electrochim. Acta 105 (2013) 157–161.
[41] C. Chen, F. Chen, L. Zhang, S. Pan, C. Bian, X. Zheng, X. Meng, F.S. Xiao, Importance of platinum particle size for complete oxidation of toluene over Pt/ZSM-5 catalysts, Chem Commun. 51 (2015) 5936–5938.
[42] Q. Chen, J. Chen, C. Gao, M. Zhang, J. Chen, H. Qiu, Hemin-functionalized WS_2 nanosheets as highly active peroxidase mimetics for label-free colorimetric detection of H_2O_2 and glucose, Analyst 140 (2015) 2857–2863.